

Phase-Transition- and Dissipation-Driven Budding in Lipid Vesicles

Thomas Franke,^[a] Christian T. Leirer,^[a] Achim Wixforth,^[a] Nily Dan,^[b] and Matthias F. Schneider*^[a, c]

Dedicated to Erich Sackmann on the occasion of his 75th birthday

Membrane budding has been extensively studied as an equilibrium process attributed to the formation of coexisting domains or changes in the vesicle area-to-volume ratio (reduced volume). In contrast, non-equilibrium budding remains experimentally widely unexplored, especially when timescales fall well below the characteristic diffusion time of lipids, τ . We show that localized mechanical perturbations, initiated by driving giant unilamellar vesicles (GUVs) through their lipid main phase transition from the gel to the fluid phase, lead to the immediate formation of rapidly growing, localized, non-equilibrium buds when the transition takes place at short timescales ($< \tau$). We show that these buds arise from small fluidlike per-

turbations and grow as spherical caps in the third dimension, since in-plane spreading is obstructed by the continuous rigid gel-like matrix. Accounting for membrane and bulk viscosity, we demonstrate that dissipation favors the formation of multiple buds which decrease in size with increasing bulk viscosity. Above a certain critical rate of area change, which we experimentally control by the change in temperature, the dissipative contribution to the total energy of the system exceeds the elastic contributions and multiple budding is expected. This rate depends on membrane and media viscosity and is correctly predicted, in order of magnitude, by our theoretical description.

1. Introduction

Lipid bilayer membranes are “soft” two-dimensional objects with a width of about 4 nm and an area in the order of 10^6 – 10^{10} nm². Upon heating, many lipid membranes undergo a transition from a rigid gel phase to a flexible fluid phase with a bending modulus of the order of $\kappa \approx 15k_bT$.^[1] Due to their high flexibility, fluid lipid membranes display intensive shape fluctuations, which have been studied thoroughly from both a theoretical and an experimental perspective.^[1–3]

The formation of membrane ‘buds’, which are spherical protrusions extending out of the membrane plane, is a key step in cellular *endo*- and *exocytosis*. Qualitatively, similar transitions have been described in model systems as a global shape transformation^[3–5] as well as a consequence of intermembrane domain formation in a multi-component, fluid–fluid phase-separated system.^[6–7] The driving force for bud formation in these systems is thought to be the formation of minority domains in a continuous phase matrix, giving rise to a line tension penalty. Escape of the domain into the third dimension (out of the plane) reduces the contact line, and thus the associated line tension penalty.^[8] Morphological transitions in these systems were induced using different experimental methods, such as osmotic,^[3] by detergents,^[9] as well as by temperature,^[3,10] and the resulting buds grew on in the range of seconds^[10] to minutes.^[4]

In biology, however, small membrane deformations are expected to result from localized perturbations in the lipid bilayer properties and are therefore more conveniently described as a non-equilibrium process.^[11–12] As a consequence, budding transitions have been studied theoretically in terms of dynamic

processes.^[12–14] Experimentally, however, only a single work is known to the authors which reports on the dynamics of budded vesicles following a temperature jump.^[10] In contrast to our work, the timescale of the observed process is of the order of seconds, the typical relaxation time of the system.


Herein, we demonstrate that rapid heating of giant unilamellar lipid vesicles (GUVs) from their gel-to-fluid phase leads to the formation of dynamic, non-equilibrium buds. The time period of bud formation exceeds the typical timescale (diffusion time) of the system by at least an order of magnitude, which emphasizes that this is a force-driven process. The subsequent relaxation into the global equilibrium shape takes place on the same timescale as reported earlier.^[10] A theoretical approach following Sens^[12] reveals that, while the number of

[a] Dr. T. Franke,[†] Dr. C. T. Leirer,[†] Prof. A. Wixforth, Prof. M. F. Schneider
University of Augsburg, Experimental Physics I
86159 Augsburg (Germany)
Fax: (+49) 821-5983227
E-mail: matthias.schneider@physik.uni-augsburg.de

[b] Prof. N. Dan
Drexler University
Department of Chemical and Biological Engineering
Philadelphia (USA)

[c] Prof. M. F. Schneider
Boston University
Department of Mechanical Engineering, Boston, MA (USA)
E-mail: matschnei@gmail.com

[[†]] These authors contributed equally to this work.

 Supporting information for this article is available on the WWW under <http://dx.doi.org/10.1002/cphc.200900658>.

buds increases with increasing heating rate and bulk viscosity, the size of the transient buds follows exactly the opposite relation. The reason is that while dissipation favors multiple small buds, elastic processes favor single bud formation. This is in excellent agreement with our observations.

Materials and Methods

The compounds 1,2-dipalmitoyl-*sn*-glycero-3-phosphocholine (DPPC), 1,2-dimyristoyl-*sn*-glycero-3-phosphocholine (DMPC), 1,2-dipentadecanoyl-*sn*-glycero-3-phosphocholine (D₁₅PC) and 1,2-dilauroyl-*sn*-glycero-3-phosphocholine (DLPC) were purchased from Avanti Polar Lipids (Alabaster, Alabama, USA) and used without further purification. Fluorescently labeled T-Red DHPE (Texas Red 1,2-dihexadecanoyl-*sn*-glycero-3-phosphoethanolamine, triethylammonium salt) was obtained from Invitrogen/Molecular-Probes (Carlsbad, Ca) and Dil₁₈ from Sigma Aldrich (Germany). For all experiments, ultrapure water (18.2 MΩ, pure Aqua, Germany) was used.

Vesicles were prepared by a standard electroformation method.^[15] Briefly, lipid solutions containing 0.2% fluorescent dye were spread on indium tin oxide (ITO) coated glass slides and dried from organic solvent (chloroform). The remaining solvent was removed in a vacuum desiccator for at least three hours. Two ITO plates were assembled in parallel and separated by a Teflon spacer of 2 mm thickness. To initiate, lipid swelling medium was added to the films and after subsequent application of an alternating electric field of a frequency of 10 Hz and an amplitude of 1 V mm⁻¹, giant unilamellar vesicles (GUVs) formed within six hours. The GUVs were carefully transferred with a pipette into the experimental chamber containing the same iso-osmotic solution as the preparation chamber. Both fluorescent and phase-contrast images were collected with a standard charge-coupled device (CCD) camera (Hamamatsu Photonics Deutschland, Herrsching am Ammersee, Germany) coupled to an Axiovert 200 M microscope (Zeiss, Oberkochen, Germany). Our experiments were performed in a closed, temperature-controlled chamber with optical access from the bottom and the top. During the experiments, the temperature was controlled with the aid of a standard heat bath (Julabo, Seelbach, Germany), and temperature measurements were performed with a thermocouple within the experimental chamber.

2. Results

We observed the phase-transition-induced budding of a DPPC

vesicle (GUV) immersed in a narrow gap between two heated glass slides, as shown in Figure 1. The initial, wrinkled structure is typical for vesicle membranes in the gel-like phase where lipid mobility is suppressed. Increasing the temperature above the transition temperature leads to some flattening of the membrane surface and the immediate appearance of small domains (or buds), whose area grows as shown in Figure 2. The time-averaged rate of bud-area increase is estimated to be $\dot{A}_{\text{bud}} \approx 3 \cdot 10^{-10} \text{ m}^2 \text{ s}^{-1}$ from measuring the bud-radius dependence on time.

Generally, the transition into the fluid phase is associated with an area increase of about 20–25%.^[6] Considering the size of the vesicle in our experiment, this corresponds to a total change in membrane area during melting of approximately $\Delta A_{\text{tot}} \approx 3 \cdot 10^{-9} \text{ m}^2$ (calculated from the vesicle in the fluid phase because there wrinkles are absent) over a temperature interval of $\Delta T_m \approx 1^\circ \text{C}$. At an experimentally controlled heating rate of 5°C s^{-1} , we end up with a rate of change in area of $\lambda \approx 10^{-8} \text{ m}^2 \text{ s}^{-1}$ for the entire vesicle shown in Figure 1. Dividing this externally “forced” increase in area λ by the observed average area growth rate \dot{A}_{bud} of an individual bud (Figure 2) demands that the total area increase ΔA_{tot} is accommodated by

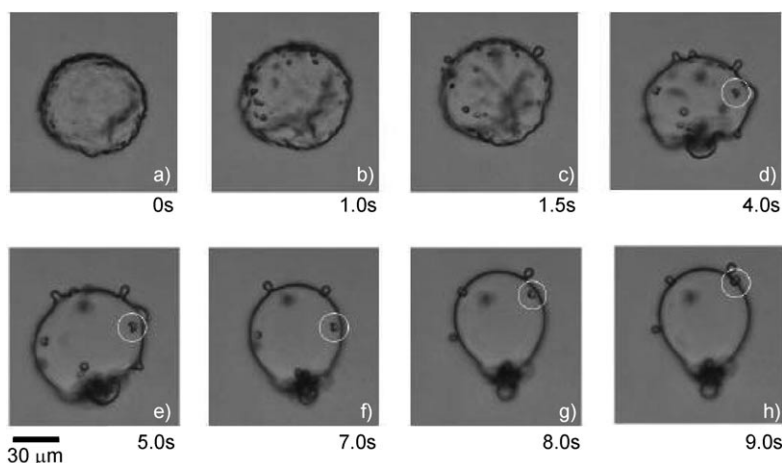


Figure 1. Phase-transition-induced extravesicular budding of pure DPPC vesicles: as the temperature is increased from $T = 35$ to 45°C , the vesicle undergoes a phase transition from gel (a) to the fluid state (b–d). The temperature of the gel–fluid phase transition of DPPC is $T_m \approx 41^\circ \text{C}$. Clearly, small buds of a final size ranging between $R \approx 1\text{--}4 \mu\text{m}$ ($R = 2.8 \pm 1.4 \mu\text{m}$) depart from the mother vesicle and disappear again. The marks in (d)–(f) point out that, originally, there is no diffusion of the buds on the vesicle surface (see the movie in the Supporting Information). Repeating experiments revealed that more than 30% of all the (freshly prepared) vesicles undergoing a morphological transition in the first place did exhibit a budding transition of the same time and size scale as presented. Buds of 23 vesicles (each between 20–40 buds) were analyzed to extract an average growth rate of $\dot{A}_{\text{bud}} \approx 3 \cdot 10^{-10} \text{ m}^2 \text{ s}^{-1}$.

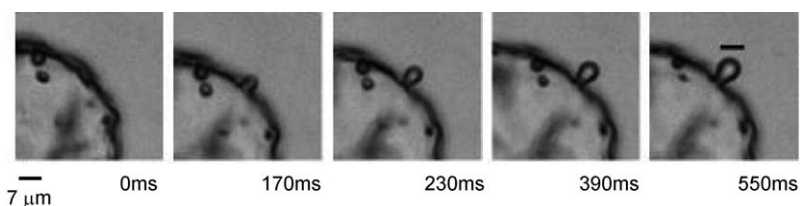


Figure 2. The dynamics of bud growth. Analyzing 50 buds, an average growth rate of $(1\text{--}3) \cdot 10^{-10} \text{ m}^2 \text{ s}^{-1}$ has been calculated (scale bar $7 \mu\text{m}$).

the formation of roughly 30 buds, which is in good agreement with our experiments where we typically found 20–40 buds (Figure 1). It shows that most of the area increase due to the melting process is consumed by formation of the microscopically visible buds. During the melting process, the surrounding of the buds becomes more fluid and therefore expands as well. For our estimate, however, we assume that the entire increase in membrane area is contained within the buds, which is supported by the observation that the buds initially formed do not show any diffusion (Figure 1d–f), which indicates a “rigid” matrix. This suggests that the process is controlled by the viscous properties of the system, and therefore, dynamical aspects also have to be incorporated. Furthermore, all buds appear as individual objects and are triggered by local rather than global changes in the membrane properties, in contrast to earlier studies on GUV vesicles from 1-stearoyl-2-oleoyl phosphatidylcholine (SOPC) and bovine brain lipids.^[3–4] All the vesicles undergo an area increase of 20–25%. However, it is important to note that not all vesicles exhibit a budding transition when heated. Approximately 30% of all (freshly prepared) vesicles showing a transition did exhibit a budding transition of the same time and size scale as presented. However, recalling that this is a dynamic process that depends on local curvature, local rate of expansion, and so on, it is not at all surprising that there is more than just one budding scenario. We believe that the reason that not all vesicles undergo the same transition is a fingerprint of uncontrollable asymmetries in lipid distribution between the inner and outer monolayer or multilayer formation, which in turn changes the spontaneous curvature. In multiple-component systems, variations in lipid distribution becomes increasingly hard to be experimentally controllable.

In the next section, we will clarify the nucleation process of the growing buds which is necessary to analyse the dynamics of the process.

2.1. Fluid Domains and Bud Nucleation

It is well-known that small fluidlike domains nucleate in a gel-like matrix during lipid main phase transition.^[17] As inferred from particle-tracking data of single buds, there is no significant diffusion of buds on the vesicle membrane. This fact supports the constellation of a gel-like majority phase with nucleating fluidlike domains. To determine whether the buds are indeed fluid, we added a small (0.1 mol%) amount of the fluorescently labelled lipid DiI18, which preferentially incorporates into the gel-phase (18). In Figure 3, a series of fluorescence images taken during the heating process of a DLPC–D₁₅PC (1:1) mixture is shown. The darker areas in the images indicate a lower dye solubility (note, however, that the dye solubility in the fluid phase is not zero), and therefore, a predominately fluid phase. This supports the idea that growing fluidlike domains in a gel-like matrix are indeed the origin of the observed buds in Figures 1 and 2. After nucleation, the melting process and accompanied area increase continues. As noted earlier, the membrane area in the fluid phase increases by approximately 25%.^[16] However, no water permeation takes place over the

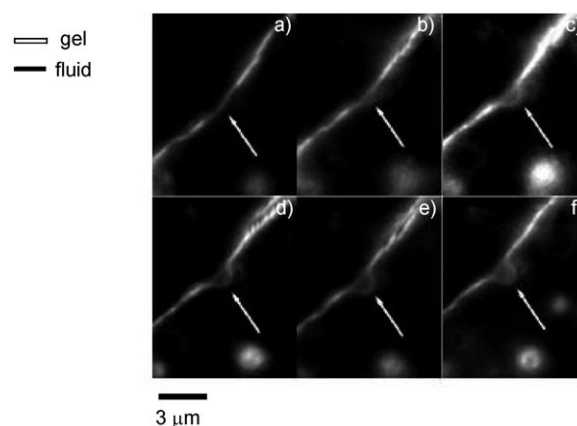


Figure 3. Fluorescence image of a section of a GUV showing bud formation. DiI18 preferentially incorporates into the gel phase and the fluid phase is therefore darker. This reveals that the bud does in fact originate from a fluidlike domain. To follow the process, experiments were performed by slowly increasing the temperature in a DLPC–D₁₅PC (1:1) mixture from 20 to 45 °C. The rather broad phase-transition regime allows us to maintain the coexistence over a longer time period. Time intervals between images were 1–2 s.

short timescales studied, constraining the overall vesicle volume. Therefore, the increase in total area results from the rapidly growing fluidlike domains, which are surrounded by a mechanically rigid gel-like matrix, and leads to a projection out of the vesicle plane, as sketched in Figure 4.

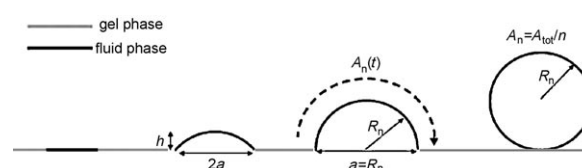


Figure 4. Domain growth under lateral confinement. The surrounding gel-like matrix does not expand during melting of the fluid domain. The increase in area due to melting requires an escape in the third dimension, thus forming a spherical cap. The height of the cap—and therefore the contact angle—is set by the projected area of the domain (namely, the area of the gel phase that transitioned into the fluid phase) and the area ratio between the fluid and gel phases, as shown in Equation (1).

2.2. Dynamics of Bud Formation

Previous experimental studies examined budding on timescales of a few seconds to minutes.^[3,4–10] Herein, however, the change in area takes place very rapidly, which leads to the formation of single buds of a diameter of about 1 μm during approximately 60 ms. Recalling that typical timescales of bulk and membrane diffusion are in the range of seconds on these size scales,^[1–4] we expect dissipation to be a major contribution to the dynamics of the morphological change. A thorough theoretical model of the dynamics of the budding process is beyond the scope of this work. In principle, our theory does not distinguish between intra and extravascular budding. A local asymmetry between the inner and outer monolayer may create a localized change in spontaneous curvature which will

favor either one of the two budding scenarios. Variations between the inner and outer side of the membrane in lipid composition, bath conditions or protein (e.g. cytoskeleton) anchoring, render this asymmetry quite likely.^[19] However, we briefly discuss the role of dissipative terms, following the work of Sens,^[12] who studied non-equilibrium bud formation due to introduction of a local change in lipid density on one side of a lipid bilayer. Although in our experiments budding is not induced by a local perturbation in lipid symmetry between the two leaflets of the bilayer membrane as in Sens work, the proposed analysis of energy dissipation still holds for our experimental situation. The change in energy E_{tot} due to the overall increase in area ΔA_{tot} during the lipid phase transition is given by the sum of the elastic (bending) and dissipative terms [Eq. (1)]:

$$E_{\text{tot}} = n\varepsilon_{\text{B}} + n \int P^{\text{Dis}} dt \quad (1)$$

where n is the number of individual buds formed and P the dissipated power. The elastic contributions ε_{B} of each individual bud are simply described by the membrane bending energy according to Helfrich^[20] [Eq. (2)]:

$$\varepsilon_{\text{B}} = \frac{\kappa}{2} \int \left(\frac{2}{R}\right)^2 dA \quad (2)$$

where κ is the bending modulus, A the area, and R_n the radius of the formed spherical cap (Figure 4). The dissipative term has two contributions: One arising from the flux of volume^[12] [Eq. (3)]:

$$P_{\text{bulk}} = \frac{22}{5} \eta \frac{(\dot{V})^2}{\pi a^3} \quad (3)$$

and a second one from the flux of membrane area [Eq. (4)]:

$$P_{\text{mem}} = \mu \frac{(\dot{A})^2}{\pi a^3} \quad (4)$$

Here, η represents the bulk viscosity, and \dot{V} and \dot{A} the change in volume and area, respectively. The parameter a denotes the neck radius of the bud and μ the lateral membrane viscosity. The fact that only fluid parts of the membrane exhibit budding allows us to treat these terms like a homogenous fluid system.

Using a Lagrangian description, Sens derived the dynamic equation for bud formation using Equations (2) and (3). However, it will turn out sufficient for our discussion to focus on the impact of n , the number of buds, and the rate of increase in total vesicle area $\lambda = dA(t)/dt$ on the total energy E_{tot} [Eq. (1)], which can be calculated as follows:

Assuming all n buds end up in the same shaped spherical shape with radius R_n (Figure 4), the elastic contribution [Eq. (2)] becomes simply $E_{\text{B}} = n\varepsilon_{\text{B}} = n8\pi\kappa$. In order to calculate the dissipation and its dependence on the rate of area increase, we need to describe the volume of the spherical cap as a function of the constant radius R_n and the momentary area of the cap $A_n(t)$ (Figure 4) [Eq. (5)]:

$$V_n = \frac{1}{3} R_n A_n(t) \quad (5)$$

with the time derivative [Eq. (6)]:

$$\dot{V}_n = \frac{1}{3} R_n \dot{A}_n(t) = \frac{1}{3} R_n \frac{\lambda}{n} \quad (6)$$

Inserting this result into Equation (3) results in the dissipated power of the bud [Eq. (7)]:

$$P_{\text{bulk}} = \frac{44}{45} \eta \lambda^2 (n^{3/2} \Delta A_{\text{tot}}^{1/2} \pi^{1/2})^{-1} \quad (7)$$

where $a \approx R_n$ and $\Delta A_{\text{tot}} = nA_n = n4\pi R_n^2$ have been used. In reality, as $a \leq R_n$, this term represents a lower limit of the dissipated energy per time, but should produce at least the order of magnitude correctly. Finally, integrating Equation (7) over the entire time of bud evolution $t_{\text{tot}} = \Delta A_{\text{tot}}/\lambda$, and accounting for the fact that volume flux takes place on the inner and outer side of the bud, we arrive at the energy dissipated by volume flux [Eq. (8)]:

$$\varepsilon_{\text{bulk}}^{\text{Dis}} = \frac{88}{45} \eta \lambda \frac{\Delta A_{\text{tot}}^{1/2}}{n^{3/2} \pi^{1/2}} \quad (8)$$

or for all n buds [Eq. (9)]:

$$E_{\text{bulk}}^{\text{Dis}} = n\varepsilon_{\text{bulk}}^{\text{Dis}} = \frac{88}{45} \eta \lambda \frac{\Delta A_{\text{tot}}^{1/2}}{n^{1/2} \pi^{1/2}} \quad (9)$$

Following the same path and using the same approximations, the energy contribution due to area flux results in Equation (10):

$$E_{\text{mem}}^{\text{Dis}} = \mu \lambda \Delta A_{\text{tot}} \quad (10)$$

or, by using Equation (1), in Equation (11):

$$E_{\text{tot}} = n8\pi\kappa + \frac{88}{45} \eta \lambda \frac{\Delta A_{\text{tot}}^{1/2}}{n^{1/2} \pi^{1/2}} + \mu \lambda \Delta A_{\text{tot}} \quad (11)$$

where $\Delta A_{\text{tot}} = 0.25 \cdot A_{\text{gel}}$ was applied.

In Figure 5, we plot the results of Equation (11) for different numbers n of buds and bulk viscosities η as a function of the growth rate λ . For small velocities, the dissipative terms do not contribute significantly and a single bud is the most likely state. Upon increasing λ , and therefore increasing dissipation, the formation of multiple buds becomes more likely. This effect is even more pronounced when the media viscosity is higher, because bulk dissipation is increased, as can be seen from Equation (7).

The model presented here suggests that under dynamic, non-equilibrium conditions, increasing media viscosity supports the formation of multiple, small buds. This is experimentally confirmed and can be seen when comparing bud formation in $\eta \approx 0.001$ Pa s (Figure 1) with bud formation when $\eta \approx 0.05$ Pa s (Figure 6). Clearly, despite the low heating rate of 5°C min^{-1} , which favors small bud formation, more buds are formed under high media viscosity conditions. Quantitatively, a

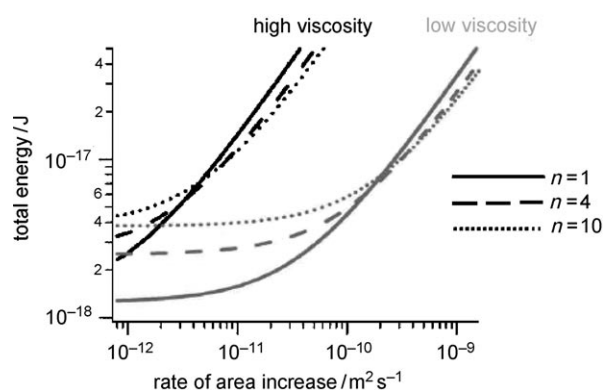


Figure 5. Plot of Equation (11) at different media viscosities and for different numbers of buds n . Changing the area per molecule at a rate above $\approx 10^{-10} \text{ m}^2 \text{ s}^{-1}$ leads to the formation of multiple buds to minimize energy dissipation. When the media viscosity is increased from 1 to 50 MPa, the rate at which dissipation dominates the system is drastically decreased to about $10^{-12} \text{ m}^2 \text{ s}^{-1}$.

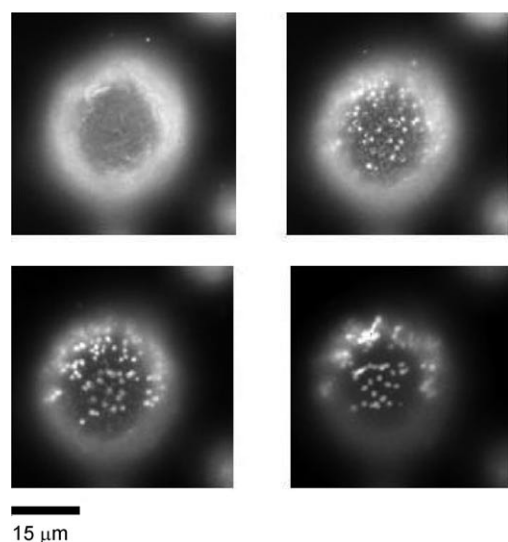


Figure 6. Bud formation is increased in a GUV of DMPC/DPPC under high media-viscosity (50 MPa) conditions using a glucose polymer (Dextran 400, Sigma Aldrich, Germany). The rate of area increase was $\lambda \approx 5 \cdot 10^{-11} \text{ m}^2 \text{ s}^{-1}$. Apart from the formation of more individual buds, the bud size is decreased roughly to the limit of optical resolution.

transition width of $\Delta T_m \approx 5^\circ \text{C}$ (DMPC/DPPC) at a heating rate of $5^\circ \text{C min}^{-1}$ leads to a rate of expansion $\lambda \approx 5 \cdot 10^{-11} \text{ m}^2 \text{ s}^{-1}$ as opposed to $\lambda \approx 10^{-8} \text{ m}^2 \text{ s}^{-1}$ for the low-viscosity experiment (Figure 1). Comparing λ for the high- and low-viscosity case to the model predictions (see Figure 5), we find that our simple non-equilibrium description correctly predicts the formation of multiple individual buds as in fact observed during our experiments. In this context, it is important to note that in biology, intracellular trafficking takes place under higher media viscosity. Kuimova et al. very recently reported a media viscosity around $\eta \approx 0.08 \text{ Pa s}$ in human ovarian cells,^[21] a value very close to the viscosity used in our experiments.

2.3. Relaxation

We consider fluid bud formation in a gel matrix as a non-equilibrium phenomenon, since a local perturbation can not relax within the membrane plane. The excess area due to the transition from gel to fluid phase must extend out of the vesicle's plane. However, as the melting progresses, the entire membrane becomes more fluid, and the vesicle is free to relax into its equilibrium state defined by the minimal bending energy^[5] at a fixed area-to-volume ratio (reduced volume ≈ 0.7). A typical relaxation process following non-equilibrium budding is shown in Figure 7. After a temperature jump, many buds arise on the surface of the vesicle. When melting is complete, the buds are re-absorbed into the membrane plane (see also Figure 1 d–g) leading to a global change in the vesicles morphology defined by its minimal bending energy. Here, the vesicle relaxes into a spherocylindrical shape as expected from a reduced volume of $v_{\text{red}} \approx 0.7$ before leaving the focus of the objective.

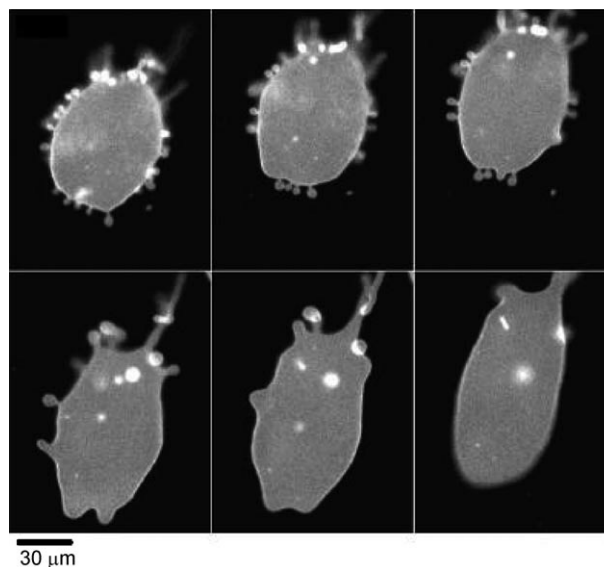


Figure 7. After complete melting ($\approx 35 \text{ s}$), the buds start to reintegrate. Since the volume of the vesicle is constant, we arrive at a new area-to-volume ratio. The reduced volume in this case is $v_{\text{red}} \approx 0.7$ (DPPC + T-Red at $\lambda \approx 10^{-8} \text{ m}^2 \text{ s}^{-1}$).

In conclusion, we present experimental evidence for a thermodynamically driven non-equilibrium budding transition in single and multi-component GUVs undergoing a transition from the gel to the fluid phase. We were able to demonstrate that the immediate evolution of localized fluidlike buds in a gel-like matrix arises as a consequence of minimal dissipation and the local mechanical properties, and are not due to global changes in the lipid membrane. The corresponding timescales exceed the diffusion limit, thereby underlining the fact that this is a force-driven process.

By increasing the media viscosity to at least more relevant intracellular media conditions,^[21] we demonstrate that our theoretical description is in good qualitative agreement with the rate of area perturbation necessary for non-equilibrium

bud nucleation. In this context it is important to note that most intracellular water is in the close vicinity of a surface, which strongly increases its viscosity.^[22] Finally, we point out that the interpretation of our findings—being caused by the physical properties of localized microdomains and their surrounding matrix—is not likely to make this of less biological relevance. Biological membranes are highly heterogeneous,^[23] dynamic systems with local changes in composition and order, and therefore, also in their mechanical properties. Such changes can trigger not only budding of lipid vesicles, as described, but also fission of lipid membranes, as has been shown recently.^[24] However, in biology the appropriate trigger may rather be protein adsorption (or binding), or pH changes, instead of temperature changes.

Acknowledgements

Financial support is acknowledged from the DFG (SFB 486), the Cluster of Excellence via NIM, the BMBF, and the Elite Netzwerk Bayern (Complnt). MFS and C.L. acknowledge their support by the Bayerische Forschungstiftung.

Keywords: budding · equilibrium · membranes · phase transitions · vesicles

- [1] "Structure and Dynamics of Membranes", E. Sackmann in *From Vesicles to Cells*. (Eds.: E. Sackmann, R. Lipowsky), Elsevier, Amsterdam, **1996**.
 [2] R. Lipowsky, *Nature* **1991**, 349, 475–481.

- [3] H. G. Döbereiner, J. Käs, D. Noppl, I. Sprenger, E. Sackmann, *Biophys. J.* **1993**, 65, 1396–1403.
 [4] H.-G. Döbereiner, E. Evans, U. Seifert, M. Wortis, *Phys. Rev. Lett.* **1995**, 75, 3360.
 [5] L. Miao, U. Seifert, M. Wortis, H.-G. Döbereiner, *Phys. Rev. E* **1994**, 49, 5389.
 [6] F. Julicher, R. Lipowsky, *Phys Rev Lett.* **1993**, 70, 2964–2967.
 [7] T. Baumgart, S. T. Hess, W. W. Webb, *Nature* **2003**, 425, 821–824.
 [8] K. Towles, N. Dan, *Biochim. Biophys. Acta* **2008**, 1778, 1190–1195.
 [9] G. Staneva, M. Seigneuret, K. Koumanov, G. Trugnan, M. I. Angelova, *Chem. Phys. Lipids* **2005**, 136, 55–66.
 [10] L. Li, X. Liang, M. Lin, F. Qiu, Y. Yang, *J. Am. Chem. Soc.* **2005**, 127, 17996–17997.
 [11] L. V. Chernomordik, M. M. Kozlov, *Nat. Struct. Mol. Biol.* **2008**, 15, 675.
 [12] P. Sens, *Phys Rev Lett.* **2004**, 93, 108103–108101.
 [13] B. Hong, F. Qiu, H. Zhang, Y. Yang, *J. Phys. Chem. B* **2007**, 111, 5837.
 [14] P. B. S. Kumar, G. Gompper, R. Lipowsky, *Phys. Rev. Lett.* **2001**, 86, 3911.
 [15] M. I. Angelova, D. S. Dimitrov, *Faraday Discuss. Chem. Soc.* **1986**, 81, 303.
 [16] T. Heimburg, *Biochim. Biophys. Acta* **1998**, 1415, 147–162.
 [17] O. G. Mouritsen, *Chem. Phys. Lipids* **1991**, 57, 179–194.
 [18] E. A. Hac, M. H. Seeger, M. Fidorra, T. Heimburg, *Biophys. J.* **2005**, 88, 317–333.
 [19] A. Iglič, H. Hagerstrand, *Med. Biol. Eng. Comp.* **1999**, 37, 125.
 [20] W. Helfrich, *Z. Naturforsch* **1973**, 28, 693–703.
 [21] M. K. Kuimova, G. Yahioglu, J. A. Levitt, K. Suhling, *J. Am. Chem. Soc.* **2008**, 130, 6672–6673.
 [22] J. S. Clegg, *J. Cell Biol.* **1984**, 99, 167s–171s.
 [23] G. Ole, K. J. Mouritsen, *BioEssays* **1992**, 14, 129–136.
 [24] C. Leirer, B. Wunderlich, V. M. Myles, M. F. Schneider, *Biophys. Chem.* **2009**, 143, 106–109.

Received: August 19, 2009

Revised: September 28, 2009

Published online on October 14, 2009